Stiffness and Transparency of a Collaborative Cable-Driven Parallel Robot

Marceau Métillon, Camilo Charron, Kévin Subrin, Stéphane Caro

Stiffness and Transparency of a Collaborative Cable-Driven Parallel Robot

Marceau Métillon, Camilo Charron, Kévin Subrin, Stéphane Caro

Abstract The subject of this paper is about the relationship between the stiffness and the transparency of Cable-Driven Parallel Robots (CDPRs) used as human-machine interfaces in object comanipulation tasks. An index quantifying the transparency of a CDPR is first introduced. The stiffness of the robot is determined in simulation which parameters have been experimentally identified. Particular attention is paid to the effect of the Moving-Platform pose and cable tension management on CDPR stiffness. Then, the relationship between the stiffness and the transparency is analysed. Finally, the transparency index is traced throughout the constant-orientation static workspace and throughout the cable tension feasibility polygon for a given MP pose.

Key words: Cable-Driven Parallel Robot, Stiffness, Collaboration, Transparency

1 Introduction

A CDPR is a particular type of parallel robot. A Moving-Platform (MP) is connected to a rigid base frame using cables. The cables are coiled around motorized winches

Marceau Métillon
Centre National de la Recherche Scientifique (CNRS), LS2N, Nantes, 44300 France
e-mail: marceau.metillon@ls2n.fr
Camilo Charron
Université de Rennes 2, Rennes, 35043 France
e-mail: camilo.charron@ls2n.fr
Kévin Subrin
Nantes Université, Carquefou, 44470 France
e-mail: kevin.subrin@ls2n.fr
Stéphane Caro
Centre National de la Recherche Scientifique (CNRS), LS2N, Nantes, 44300 France
e-mail: stephane.caro@ls2n.fr

which control the cable lengths therefore translating and orientating the MP. Cable routing is made from the winches to the anchor points on the MP via exit points located on pulleys attached to the base frame. CDPRs are advantageous for industrial applications such as intra-logistics manipulation [4], large scale 3D printing [1], manipulation of large and/or heavy parts [14] and search-and-rescue operations [11].

When an external wrench is applied to the MP, cables exhibit an elastic behaviour and the MP tends to move further from its static equilibrium pose. The stiffness analysis of a CDPR is crucial to predict the MP displacement due to an external wrench resulting from its weight or a collision with its environment. Several papers deal with CDPR stiffness analysis [2, 16] for CDPR design [3] or control [5, 13]. In the field of Human-Robot Interactions, the interaction transparency has different meanings depending on the nature of the interaction. Considering non-physical interactions between a human user agent and a robotic agent, the transparency describes the reciprocal knowledge of the other agent intentions [10]. Considering physical Human-Robot Interactions (pHRI) in the field of bilateral teleoperation, the transparency index is defined as the system capacity of rendering the interacting environment impedance [9]. In the field of comanipulation, where the robotic system is granting a manipulation assistance to the user, the transparency of the interaction denotes the capacity of the robot to moves in the direction desired by the user [8]. This definition is used in this paper to characterize the transparency. The paradigm of pHRI involving a human user and a CDPR is considered as shown in Fig 1(a).

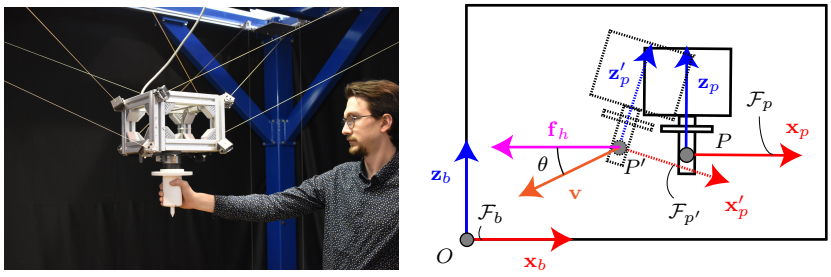

(a) Human user interacting with a CDPR

(b) Transparency

Fig. 1: Physical Human-Robot Interaction with a Cable-Driven Parallel Robot - LS2N, Nantes, France

The MP is equipped with a handle that the user grabs and exert wrench onto to infer motion intention. A force/torque sensor mounted between the MP and the handle measures the wrench exerted by the user. An admittance control strategy converts the measured wrench into a desired acceleration of the MP for the robot to servo [7]. As the user is exerting wrench on the MP the latter is subject to displacements that can affect the wrench measurement therefore impacting the motion direction of the robot thus affecting the transparency. Works have been done on the link between stiffness and transparency in teleoperation paradigms [15] but to the best of the

authors knowledge, no study has been conducted on the effect of the stiffness of a CDPR on its transparency when used as a human-robot interface in a comanipulation task. As a consequence, this paper deals with the analysis of the effect of: (*i*) the cable tension distribution and the MP pose on the CDPR stiffness; (*ii*) the CDPR stiffness on its transparency when used as an interface in a human-robot comanipulation task. Section 2 describes the stiffness models of the CDPR under study. Section 3 presents the results on the stiffness analysis. A novel transparency index is introduced and analysed in Section 4 as well as the effect of stiffness on transparency. Conclusions and future work are drawn in Section 5.

2 CDPR stiffness modelling

From [2] and [13], the Cartesian stiffness matrix of a CDPR can be expressed as:

$$\mathbf{K} = \mathbf{K}_a + \mathbf{K}_p \tag{1}$$

with $\mathbf{K}_a$ being the active stiffness matrix and $\mathbf{K}_p$ being the passive stiffness matrix.

The passive stiffness matrix is dependent on the MP pose and the cable elasticity so that:

$$\mathbf{K}_p = \sum_{i=1}^{m} k_i \begin{bmatrix} {}^b\mathbf{u}_i\,{}^b\mathbf{u}_i^\mathsf{T} & {}^b\mathbf{u}_i\,{}^b\mathbf{u}_i^\mathsf{T}\,{}^b\hat{\mathbf{b}}_i^\mathsf{T} \\ {}^b\hat{\mathbf{b}}_i\,{}^b\mathbf{u}_i\,{}^b\mathbf{u}_i^\mathsf{T} & {}^b\hat{\mathbf{b}}_i\,{}^b\mathbf{u}_i\,{}^b\mathbf{u}_i^\mathsf{T}\,{}^b\hat{\mathbf{b}}_i^\mathsf{T} \end{bmatrix} \tag{2}$$

where k_i is the i-th cable elasticity, ${}^b\mathbf{u}_i$ is the unit cable vector denoting the i-th cable direction and ${}^b\hat{\mathbf{b}}_i$ is the cross-product matrix of the anchor point vector ${}^b\mathbf{b}_i$ expressing the coordinates of the MP anchor points in the base frame. The cable elasticity is given by $k_i = ES/l_i$ where E is the Young's modulus of the cable material, S is the cable cross-sectional area and l_i is the uncoiled cable length from the winch to the MP anchor points.

The active stiffness matrix is dependent on the MP pose, the cable lengths and the cable tensions so that:

$$\mathbf{K}_a = -\sum_{i=1}^{m} \tau_i \begin{bmatrix} -\frac{1}{l_i}\left(\mathbf{I}_3 - {}^b\mathbf{u}_i\,{}^b\mathbf{u}_i^\mathsf{T}\right) & \frac{1}{l_i}\left(\mathbf{I}_3\,{}^b\mathbf{u}_i\,{}^b\mathbf{u}_i^\mathsf{T}\right){}^b\hat{\mathbf{b}}_i^\mathsf{T} \\ -\frac{1}{l_i}\,{}^b\hat{\mathbf{b}}_i\left(\mathbf{I}_3 - {}^b\mathbf{u}_i\,{}^b\mathbf{u}_i^\mathsf{T}\right) & \left[{}^b\hat{\mathbf{u}}_i + \frac{{}^b\hat{\mathbf{b}}_i}{l_i}\left(\mathbf{I}_3 - {}^b\mathbf{u}_i\,{}^b\mathbf{u}_i^\mathsf{T}\right)\right]{}^b\hat{\mathbf{b}}_i^\mathsf{T} \end{bmatrix} \tag{3}$$

where τ_i is the i-th cable tension.

3 Analysis of factors influencing stiffness

In this section, the influence of the MP pose and tension distribution on CDPR stiffness is carried out in simulation in order to further analyse the impact on the transparency. The CDPR considered is the CRAFT prototype, located at LS2N, Nantes, of size 3.75 m x 4.34 m x 2.78 m. The prototype is equipped with eight motorized winches which have lower and upper cable tensions capacities $\boldsymbol{\tau}_{min}$ and $\boldsymbol{\tau}_{max}$ equal to 0 N and 100 N, respectively. The cables used are synthetic cables VECT070LE composed of 8 braids of Vectran® fibres[1]. The cable diameter is 0.7 mm. The cable elasticity was experimentally determined using a Universal Tensile Machine during a stress–strain analysis experiment. The identified elasticity is found to be $ES = 17318.1$ N.

To assess the evolution of the stiffness for the CRAFT prototype, the displacements of the MP under an external wrench are determined and compared. The external wrench is the wrench exerted by the user and is expressed as $\mathbf{w}_h = [\mathbf{f}_h \ \mathbf{m}_h]^\mathsf{T}$ with $\mathbf{f}_h = [-15\ 0\ 0]^\mathsf{T}$ N and $\mathbf{m}_h = \mathbf{0}_3$. The human operator exerts a pure force $\mathbf{f}_h$ at point P being located on the handle. The small-displacement screw $\delta\mathbf{X} = [\delta\mathbf{p}\ \boldsymbol{\varphi}]^\mathsf{T}$ of the MP due to force exerted by the human operator is the following:

$$\delta\mathbf{X} = \mathbf{K}^{-1}\mathbf{w}_h \tag{4}$$

with $\delta\mathbf{X}$ being the displacement of the MP in term of translation and orientation so that $\delta\mathbf{X} = [\delta\mathbf{p}\ \boldsymbol{\varphi}]^\mathsf{T}$ with $\delta\mathbf{p} = [\delta p_x\ \delta p_y\ \delta p_z]^\mathsf{T}$ and $\boldsymbol{\varphi} = [\varphi_x\ \varphi_y\ \varphi_x]^\mathsf{T}$.

3.1 Influence of the MP pose on the manipulator stiffness

From Eq. (2) and Eq. (3), both the passive and active stiffness matrices are dependent on the unit cable vectors $\mathbf{u}_i$, therefore, the stiffness of the robot varies depending of the pose. Here the influence of the pose on the stiffness is simulated. The constant and null orientation Static Workspace of the robot is determined using the Capacity Margin index [6]. Then, the static workspace is discretized and the robot stiffness is computed at each point. In this scenario, the cable tension distribution considered corresponds to the barycentre of the cable tension feasibility polygon of each pose considering the static equilibrium of the MP [12]. The displacement of the MP under the external wrench exerted by the human user is computed using the matrix $\mathbf{K}$ at each pose.

Figure 2 shows the influence of the MP pose on the robot stiffness. Figure 2(a) shows the translational displacement of the MP δp_x along $\mathbf{x}_b$ axis and Fig. 2(b) shows the MP rotational displacement φ_y around $\mathbf{y}_b$ axis. It can be seen that the robot stiffness decreases when the MP altitude is increasing and when the MP moves away from the vertical centreline of the workspace.

[1] Acquired from Corderie Lancelin, `https://www.lancelin.com/en/`

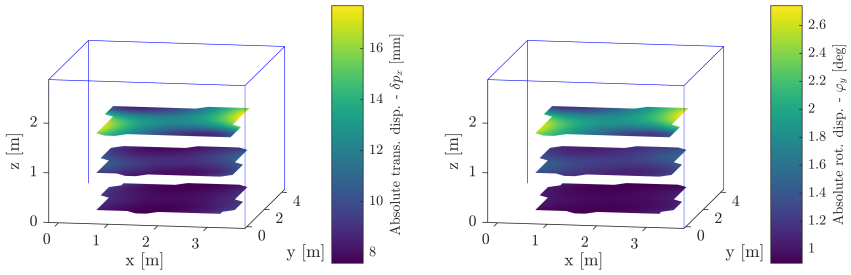

(a) Translational displacement along $\mathbf{x}_b$ (b) Rotational displacement around $\mathbf{y}_b$

Fig. 2: Displacement of the MP subject to an external wrench through the manipulator static workspace

3.2 Influence of the cable tension distribution

The static equilibrium of the MP is written as

$$\mathbf{W}\boldsymbol{\tau} + \mathbf{w}_h + \mathbf{w}_g = \mathbf{0}_8 \tag{5}$$

where $\mathbf{W}$ is the pose-dependent wrench matrix associated to the MP, $\boldsymbol{\tau}$ being the cable tension vector, $\mathbf{w}_h$ being the wrench applied by the human user on the MP and $\mathbf{w}_g$ being the gravity wrench.

The number of cables of the CDPR under study is larger than its number of degrees of freedom. Therefore an infinite number of cable tension sets exists to ensure the static equilibrium of the MP. It can be seen from Eq. (3) that the cable tensions have an influence on the overall robot stiffness. In this section the influence of the cable tension distribution is studied. The methodology to compute the cable tension feasible polygon detailed in [13] is used hereafter. The cable tension feasible polygon Λ_f is the convex polytope of $\boldsymbol{\lambda} = [\lambda_1\ \lambda_2]^\mathsf{T}$ that satisfies the static equilibrium of the MP and the cable tension limits so that:

$$\Lambda_f = \left\{\boldsymbol{\lambda} \in \mathbb{R}^2 \mid \boldsymbol{\tau}_{min} \leq \boldsymbol{\tau}_0 + \mathbf{N}\boldsymbol{\lambda} \leq \boldsymbol{\tau}_{max}\right\} \tag{6}$$

with $\boldsymbol{\tau}_0 = -\mathbf{W}^\dagger\left(\mathbf{w}_g + \mathbf{w}_h\right)$, $\mathbf{N} = \text{null}(\mathbf{W})$ being the null space of the wrench matrix. $\boldsymbol{\tau}_{min}$ and $\boldsymbol{\tau}_{max}$ are the lower and upper bound cable tension vectors, respectively. To study the influence of the cable tension distribution, the space Λ_f was numerically obtained for a given MP pose of the MP, in this case $\mathbf{p} = [1.87\ 2.15\ 0.5]^\mathsf{T}$ m. The feasible polygon is then discretized and the displacement of the MP under the external wrench is computed for each discrete point. Figure 3 shows the influence of cable tension distribution on the robot stiffness. Figure 3(a) shows the translational MP displacement δp_x along $\mathbf{x}_b$ axis and Figure 3(b) shows the MP rotational dis-

placement φ_y around $\mathbf{y}_b$ axis. The robot stiffness is maximized along $\mathbf{x}_b$ axis and around $\mathbf{y}_b$ axis for $\boldsymbol{\lambda} = [35.54 \ \ -41.9]^\mathsf{T}$.

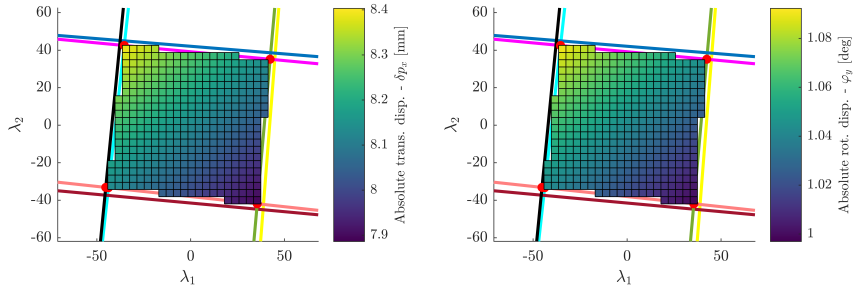

(a) Translational displacement along $\mathbf{x}_b$ (b) Rotational displacement about $\mathbf{y}_b$

Fig. 3: Effect of the cable tension distribution on the MP displacement subject to an external wrench.

4 Transparency

From [8], the transparency index describes the capacity of the robot to follow the human intention in terms of desired displacement. The user desired motion direction relies in the force direction. For the CDPR used as an assistive device, the force exerted on the sensor induces a desired acceleration of the MP based on the force direction. The transparency index μ is expressed as:

$$\mu = \mathbf{v}_n^\mathsf{T} \, \mathbf{f}_{hn} \tag{7}$$

with $\mathbf{v}_n$ being the unit vector of the MP translational velocity vector and $\mathbf{f}_{hn}$ being the unit vector of the human force $\mathbf{f}_h$. From Eq. (7), μ amounts to the cosine of angle $\theta = \angle(\mathbf{v}_n, \ \mathbf{f}_{hn})$ between vectors $\mathbf{v}_n$ and $\mathbf{f}_{hn}$

It should be noted that the CDPR stiffness affects the transparency index when used in comanipulation, especially when using an admittance control strategy based on wrenches applied on the MP. The parameters used in this section are depicted in Fig. 1(b). Equation (4) denotes the displacement of the MP under the external force due to the pose-dependant robot stiffness $\mathbf{K}$. $\mathbf{X}'$ denotes the new MP pose after small displacement. Due to this displacement, the force measurement in $\mathcal{F}_p$ is distorted due to the small rotational motion of the MP. The expression of the force measured in the sensor frame considering the displacement of the MP is obtained as:

$$\mathbf{f}_h' = {}^b\mathbf{R}_{p'} \mathbf{f}_h \tag{8}$$

with ${}^{b}\mathbf{R}_{p'}$ being the rotation matrix from frame $\mathcal{F}_b = (O, \mathbf{x}_b, \mathbf{y}_b, \mathbf{z}_b)$ and $\mathcal{F}_{p'} = (P', \mathbf{x}_{p'}, \mathbf{y}_{p'}, \mathbf{z}_{p'})$ where $\mathbf{x}_{p'} = {}^{b}\mathbf{R}_{p'}\mathbf{x}_b$, $\mathbf{y}_{p'} = {}^{b}\mathbf{R}_{p'}\mathbf{y}_b$ and $\mathbf{z}_{p'} = {}^{b}\mathbf{R}_{p'}\mathbf{z}_b$.

Using the measured force as seen by the sensor, the admittance controller defines a desired Cartesian speed set-point for the robot to reach $\mathbf{t} = [\mathbf{v}, \boldsymbol{\omega}]^{\mathsf{T}}$, with $\mathbf{v} = [v_x\ v_y\ v_z]^{\mathsf{T}}$ and $\boldsymbol{\omega} = [\omega_x\ \omega_y\ \omega_z]^{\mathsf{T}}$ being the MP translational velocity and angular velocity respectively. In this specific case only translational motions are generated using the admittance and angular velocity are kept null so that $\boldsymbol{\omega} = \mathbf{0}_3$. The speed set-point $\mathbf{t}$ is then used in the robot controller to compute the cable speed set-point $\dot{\mathbf{l}}$ using the kinematic forward Jacobian matrix $\mathbf{A}(\mathbf{X})$ such as:

$$\dot{\mathbf{l}} = \mathbf{A}(\mathbf{X})\mathbf{t} \tag{9}$$

In order to compute the transparency as the dot product of the unit vectors of the velocity and the force applied on the MP, it is necessary to determine the effective velocity of the MP by taking into account that the robot controller does not have prior knowledge of the MP displacement. Therefore, the force measured and the cable speed defined using the admittance controller will not lead to the correct robot motion. The MP velocity is obtained using the kinematic forward Jacobian matrix corresponding to the displaced pose $\mathbf{A}(\mathbf{X}')$ and the cable speed set-point issued by the controller $\dot{\mathbf{l}}$ as:

$$\mathbf{t}' = \mathbf{A}^{\dagger}(\mathbf{X}')\dot{\mathbf{l}} \tag{10}$$

with $\mathbf{A}^{\dagger}(\mathbf{X}')$ being the pseudo-inverse of the matrix $\mathbf{A}(\mathbf{X}')$ and $\mathbf{t}' = [\mathbf{v}'\ \boldsymbol{\omega}']^{\mathsf{T}}$ being the MP twist accounting for the MP displacement under external wrenches. Therefore, the transparency index μ' accounting for the CDPR stiffness can be defined as:

$$\mu' = \mathbf{v}_n'^{\mathsf{T}}\, \mathbf{f}_{hn} \tag{11}$$

where $\mathbf{v}_n'$ is the unit vector of the MP linear velocity vector, $\mathbf{v}'$.

The results on the stiffness analysis carried out in Sec. 3 are used to compute the transparency index throughout the manipulator workspace. It is then possible to apprehend the influence of the MP pose and the cable tension distribution on the transparency index. It should be noted that index μ' is bounded between -1 and 1. In order to have an index bounded between 0 and 1 and have a better assessment of the effect of the orientation error of the MP on the human user's feeling, a novel transparency index, named ν', is expressed as:

$$\nu' = e^{-k\frac{1-\mu'}{2(\mu'+1)}} \tag{12}$$

with k being a scaling factor to be tuned based on the task and the CDPR performance. ν' is bounded between 0 and 1. The higher ν', the better the transparency of the comanipulation task. Figure 4 shows the effect of the MP pose and cable tension distribution on transparency with a scaling factor $k = 500$. Figure 4(a) shows that the cable tension distribution has a negligible effect on the transparency. Due to the cable tension limits, the cable tension distribution offers a small range of controllability of the stiffness and therefore a small range of controllability of the transparency.

Figure 4(b) shows that the lower the MP, the better the transparency and that the MP pose has a preponderant effect on the transparency over the cable tension distribution.

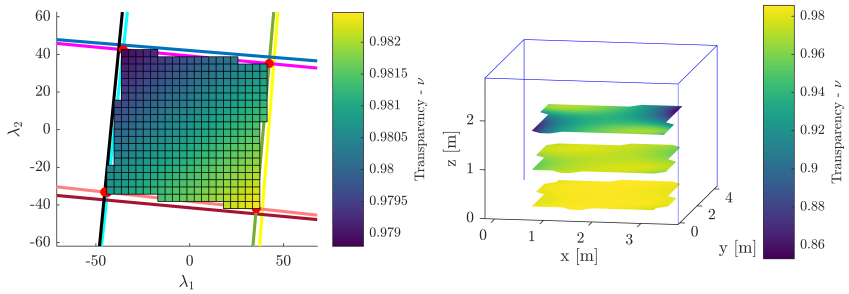

(a) Influence of the cable tension distribution

(b) Influence of the MP pose

Fig. 4: Influence of stiffness on transparency

5 Conclusion and future work

In this paper, the stiffness of the CDPR prototype CRAFT was analysed and compared based on MP pose and cable tension management. The displacement of the MP under an external pure force was studied and its impact on the robot transparency was investigated. A novel transparency index was introduced and it turns out that the transparency of the CDPR is clearly a function of its stiffness. The higher the robot stiffness, the better the transparency. Future work will focus on additional elements influencing the robot stiffness such as couplings between the motor gearboxes and the winches. The transparency analysis will be extended to multiple wrenches exerted by a human-operator on the MP and control solutions towards transparency improvement. The effect of the communication time from the force sensor to the robot control bay on the transparency will also be investigated.

Acknowledgements This work was supported by the ANR CRAFT project, grant ANR-18-CE10-0004.`https://anr.fr/Project-ANR-18-CE10-0004`.

References

1. Barnett, E., Gosselin, C.: Large-scale 3d printing with a cable-suspended robot. Additive Manufacturing **7**, 27–44 (2015). DOI 10.1016/j.addma.2015.05.001

2. Behzadipour, S., Khajepour, A.: Stiffness of cable-based parallel manipulators with application to stability analysis. Journal of Mechanical Design **128**(1), 303–310 (2006). DOI 10.1115/1.2114890
3. Bolboli, J., Khosravi, M.A., Abdollahi, F.: Stiffness feasible workspace of cable-driven parallel robots with application to optimal design of a planar cable robot. Robotics and Autonomous Systems **114**, 19–28 (2019). DOI 10.1016/j.robot.2019.01.012
4. Bruckmann, T., Lalo, W., Nguyen, K., Salah, B.: Development of a storage retrieval machine for high racks using a wire robot. In: Proceedings of the ASME International Design Engineering Technical Conferences and Computers and Information in Engineering Conference–2012, pp. 771–780. American Society of Mechanical Engineers, New York N.Y. (2012 -). DOI 10.1115/DETC2012-70389
5. Cui, Z., Tang, X.: Analysis of stiffness controllability of a redundant cable-driven parallel robot based on its configuration. Mechatronics **75**, 102519 (2021). DOI 10.1016/j.mechatronics.2021.102519
6. Guay, F., Cardou, P., Cruz-Ruiz, A.L., Caro, S.: Measuring how well a structure supports varying external wrenches. In: V. Petuya, C. Pinto, E.C. Lovasz (eds.) New advances in mechanisms, transmissions and applications, *Mechanisms and Machine Science*, vol. 17, pp. 385–392. Springer, New York (2013). DOI 10.1007/978-94-007-7485-8_47
7. Hogan, N.: Impedance control: An approach to manipulation: Part i—theory. Journal of Dynamic Systems, Measurement, and Control **107**(1), 1–7 (1985). DOI 10.1115/1.3140702
8. Jarrasse, N., Paik, J., Pasqui, V., Morel, G.: How can human motion prediction increase transparency? In: Robotics and Automation, 2008, ICRA 2008, IEEE International Conference on, pp. 2134–2139. IEEE Xplore, [Pitscataway, NJ] (2008). DOI 10.1109/ROBOT.2008.4543522
9. Lawrence, D.A.: Stability and transparency in bilateral teleoperation. IEEE Transactions on Robotics and Automation **9**(5), 624–637 (1993). DOI 10.1109/70.258054
10. Lyons, J.B.: Being transparent about transparency: A model for human-robot interaction. In: Trust and autonomous systems, Technical Report / Association for the Advancement of Artificial Intelligence SS. AAAI Press, Palo Alto, Calif. (2013)
11. Merlet, J.P., Daney, D.: A portable, modular parallel wire crane for rescue operations. In: 2010 IEEE International Conference on Robotics and Automation, pp. 2834–2839. IEEE, [Piscataway, N.J.] (2010). DOI 10.1109/ROBOT.2010.5509299
12. Mikelsons, L., Bruckmann, T., Hiller, M., Schramm, D.: A real-time capable force calculation algorithm for redundant tendon-based parallel manipulators. In: Robotics and Automation, 2008, ICRA 2008, IEEE International Conference on, pp. 3869–3874. IEEE Xplore, [Pitscataway, NJ] (2008). DOI 10.1109/ROBOT.2008.4543805
13. Picard, E., Caro, S., Plestan, F., Claveau, F.: Stiffness oriented tension distribution algorithm for cable-driven parallel robots. In: J. Lenarčič, B. Siciliano (eds.) Advances in Robot Kinematics 2020, *Springer Proceedings in Advanced Robotics*, vol. 15, pp. 209–217. Springer International Publishing, Cham (2021). DOI 10.1007/978-3-030-50975-0_26
14. Picard, E., Plestan, F., Tahoumi, E., Claveau, F., Caro, S.: Control strategies for a cable-driven parallel robot with varying payload information. Mechatronics **79**, 102648 (2021). DOI 10.1016/j.mechatronics.2021.102648
15. Roche, L., Saint-Bauzel, L.: High stiffness in teleoperated comanipulation: Necessity or luxury? In: K. Lynch (ed.) 2018 IEEE International Conference on Robotics and Automation (ICRA), pp. 477–483 (2018). DOI 10.1109/ICRA.2018.8461005
16. Yuan, H., Courteille, E., Deblaise, D.: Static and dynamic stiffness analyses of cable-driven parallel robots with non-negligible cable mass and elasticity. Mechanism and Machine Theory **85**, 64–81 (2015). DOI 10.1016/j.mechmachtheory.2014.10.010